ULTRASONIC GUIDED WAVES BASED METHOD FOR SHM – SIMULATIONS AND AN EXPERIMENTAL TEST

L. Ambrozinski
AGH-University of Science and Technology, Krakow, POLAND
lukasz.ambrozinski@agh.edu.pl

P. Packo
AGH-University of Science and Technology, Krakow, POLAND
pawel.packo@agh.edu.pl

T. Stepinski
Uppsala University, Uppsala, SWEDEN
ts@signal.uu.se

T. Uhl
AGH-University of Science and Technology, Krakow, POLAND
tuhl@agh.edu.pl

Abstract

Guided waves based methods are widely used for damage detection and localization in metallic and composite structures. Success of the method application depends on many factors like sensors/actuators location, sensor electronic system design, sensor shape, frequency range of excitation waves and applied signal processing procedures. Authors developed new modified LISA and EFIT algorithms to solve guided waves propagation problem in metallic and composite structures. Developed procedure helps to simulate wave propagation for damaged and undamaged structures for different configuration of sensors and actuators locations, shapes of sensors and frequency range. Simulation results helped to design system including hardware and software for monitoring and diagnostics of plate-like structures. Time and frequency domain methods are implemented in the system for damage detection. The simulation results have been validated using experimental test of aluminum and composite structures with different sensor/actuators configuration. New SHM system design based on formulated method and its application for real mechanical structures will be presented.

Introduction

Lamb waves are widely used in SHM applications to plate-like structures. The ability of waves to travel over long distances enables inspections of wide areas in short time. Since Lamb waves propagation is a rater complex phenomenon when a Lamb wave based SHM system is designed many factors should be taken into account.

Made up of a superposition of longitudinal and shear waves, Lamb waves can propagate in both symmetric and anti-symmetric modes. Infinite number of modes can exist in a plate. The dispersion relation can be found for isotropic materials from Rayleigh-Lamb frequency equation roots:

$$\frac{\tan(qh)}{\tan(ph)} = -\frac{4k^2qp}{\left(k^2-q^2\right)^2} \tag{1}$$

$$\frac{\tan(qh)}{\tan(ph)} = -\frac{\left(k^2-q^2\right)^2}{4k^2qp} \tag{2}$$

where: $p^2 = \frac{\omega^2}{c_L} - k^2$, $q^2 = \frac{\omega^2}{c_T} - k^2$, $k = \frac{\omega}{c_P}$, h is the plate thickness, k is wavenumber, c_L is the velocity of longitudinal wave mode, c_T is the velocity of shear wave mode, c_P is the phase velocity and ω is the circular wave frequency (Su *et al.*, 2006). Equations (1) and (2) define the symmetric and antisymmetric modes, respectively. Group velocity can be calculated from the equation:

$$c_G = \frac{\partial \omega}{\partial k} \tag{3}$$

The solution of eqs (1) and (2) is presented in Figure 2a as a wavenumber vs. frequency plot. Although many modes can be excited in a plate, for low frequencies below certain limit frequency only two modes, S_0 and A_0, exist. Wavemode selection is essential for the damage detection algorithm. Both S_0 and A_0 modes are sensitive to the structural damages, however, S_0 is more sensitive to damage in the structural thickness whereas surface cracks are easier to detect when A_0 mode used (Su and Ye, 2009)

PZTs wafers attached to the plate surface generate normally both S_0 and A_0 modes. It is possible, however, to enhance the desired mode and minimize the other by using mode tuning techniques. The method proposed by Su *et al* (2004) requires two PZTs actuators attached on both sides of the investigated plate, which is impracticable in many applications. Other method, proposed by Giurgiutiu (2005) is based on the selection of transducer size and excitation frequency.

The brief review of Lamb waves theory presented above is insufficient to design a real SHM system. Some of the problems can be solved thanks to analytical relationships but still an advanced simulation tool is needed to facilitate the design process and to facilitate the analysis of the influence of the parameter selection on wave propagation.

Numerical modeling of wave propagation

Simulations have been carried out with two modified numerical algorithms: the Local Interaction Simulation Approach / Sharp Interface Model (LISA/SIM) and the Elastodynamic Finite Integration Technique (EFIT), both implemented in 2D formulations.

LISA

To obtain LISA/SIM governing equations we are considering wave equation for homogenous, isotropic and linearly elastic material of the form:

$$(\lambda + \mu)\nabla\nabla \cdot W + \mu\nabla^2 W = \rho W_{,tt} \tag{4}$$

where λ, μ are Lame constants, ρ is material density, and W is the displacement vector with u and v components. Indices after comma denote differentiating with respect to these quantities. Assuming translational symmetry, the problem can be reduced to 2D, which results in the coupled in-plane particle motion and the decoupled out-of-plane particle motion. Following Delsanto *et al.* (1994), we divide computational domain into a grid of square cells of size *dc*, connected by nodes located in their corners. The time discretizing is performed with steps *dt*. Then, using finite difference formalism of the first order we obtain matrix equation for the displacement for the node *(i,j)* for time *t+1*:

$$W_{t+1} = 2W - W_{t-1} + dt^2 \left[\frac{A}{dc^2}(W_{i+1} + W_{i-1} - 2W) + \frac{B}{dc^2}\left(W_{j+1} + W_{j-1} - 2W\right) + \frac{C}{4dc^2}\left(W_{i+1,j+1} + W_{i-1,j-1} - W_{i-1,j+1} - W_{i+1,j-1}\right)\right] \tag{5}$$

where

$$W = \begin{pmatrix} u \\ v \end{pmatrix} \quad A = \begin{pmatrix} \lambda + 2\mu & 0 \\ 0 & \mu \end{pmatrix} \quad B = \begin{pmatrix} \mu & 0 \\ 0 & \lambda + 2\mu \end{pmatrix} \quad C = \begin{pmatrix} 0 & \lambda + \mu \\ \lambda + \mu & 0 \end{pmatrix}$$

For briefness we have omitted subscripts, whenever equal to *t*, *i* or *j*. The detailed procedure for cross points treatment leading to SIM model can be found in (Delsanto *et al.*, 1994),

EFIT

The underlying governing equations of elastodynamic waves that rely on two fundamental physical laws: the Newton`s 2nd law and the Hooke`s law, can be expressed in the form of two equations:

$$\iiint_V \rho_0 \cdot \frac{\delta}{\delta t} \underline{v}\, dV = \oiint_S \underline{\mathrm{n}} \cdot \underline{\underline{\sigma}}\, dS \tag{7}$$

$$\iiint_V \frac{\delta}{\delta t} \underline{\underline{\sigma}}\, dV = \underline{\underline{\underline{C}}} \iint_S \frac{1}{2} \left(\underline{n}\, \underline{v} + \underline{v}\, \underline{n} \right) dS \tag{8}$$

where: V is volume, $\underline{v}$ - velocity vector, $\underline{\mathrm{n}}$ - outward normal vector of the closed surface S, ρ_0 – material density, $\underline{\underline{\sigma}}$ - stress tensor of the second rank, and $\underline{\underline{\underline{C}}}$ is the stiffness tensor of the fourth rank. In the first equation the force is expressed by time derivative of linear momentum and substituted into Cauchy`s equation for the total force density acting on an elastic solid particle. In the second equation Hooke`s law and the law of deformation are combined and expressed in terms of particle velocity.

To discretize the equations, the space of interest is divided into square cells with edge length *dc*, yielding a regular grid. Volume and surface integrals from eqs (7) and (8) are evaluated approximately for each discretization volume, assuming constant velocity and stress components within volume and on each of the six quadratic surfaces of the considered cube. This requires staggered grids centered on the field components. The EFIT-v-grid and EFIT-σ-grid can be extracted from the particular integration volumes. Both grids and integration cells for velocity components are shown in Figure 1.

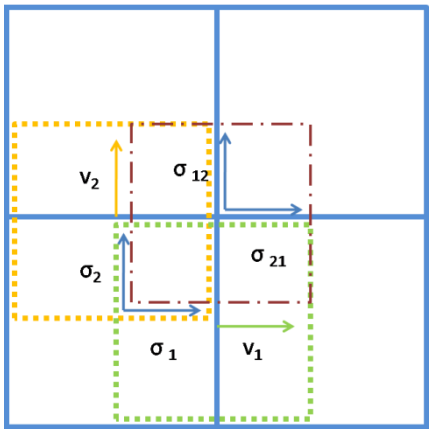

Figure 1. Staggered grid scheme for 2D EFIT algorithm. Integration cells for v_1 (dotted green cell) and v_2 (dotted orange cell) are shown.

The staggered grid allocation of the discrete field components also requires a staggered allocation in time, thus field components are calculated for full or half time steps *dt*. Detailed derivation of EFIT algorithm can be found in (Fellinger *et al.*, 1995).

SHM system design

Wave based methods enable detecting damages larger than half wavelength, thus the shorter wavelength the smaller damage can be detected by the method. The proposed simulation methods allow for the analysis of Lamb waves behavior in plate-like structures. It is possible to evaluate Lamb wave frequency characteristics in the modeled structure. Based on these predictions the appropriate excitation frequency bands can be determined and applied according to the damage size that has to be detected. It is also possible to determine the number of significant modes propagating at particular frequency.

The proposed procedure enables simulating wave propagation for different configuration of sensors and actuators. It also facilitates prediction of the influence of transducer locations on the wave pattern in the plate.

Identification of the dispersion characteristics

Determining the dispersion characteristics of the guided waves is essential for many damage detection algorithms. As mentioned above, the dispersion curves can be obtained from root-finding Rayleigh-Lamb, eq. (1). The numerical solutions can be also obtained by means of LISA and EFIT algorithms. To validate the analytically and numerically calculated curves by comparing them with the experimental ones, the 2D Fourier transform method for the measurement of propagating multimode signals was used (Alleyne and Cawley, 1991).

Both simulations were performed for 2 mm aluminum plate with Young modulus 70 GPa, Poisson ratio 0.33 and density 2.7 g/cm^3. As excitation a broadband square signal was used. Measuring points, both for simulations and experiment were placed every 1 mm in the range from 65 to 140 mm from excitation source, resulting in 76 signals. In case of LISA simulation plate had length of 1300 mm in order to minimize effects of reflections, while in case of EFIT plate was only 300 mm length due to applied numerical damping at the ends of the plate.
For the transmission a space distributed excitation was applied to the plate by selecting number of nodes at the top surface. Nodes were excited in the direction perpendicular to the plate surface with amplitudes varying among nodes to model Gaussian spatial profile of a square 5.4 mm piezoelectric wafer in both methods. Time discretization for the algorithms was adjusted according to specific conditions for each method and the analysis time was 250 μs. Receiving transducers were not modeled explicitly – the values in the mesh nodes were used as outputs.

Both methods were implemented in MATLAB software. Calculation time for LISA was approx. 22 min, while for EFIT approx. 30 min on Dual Core machine with 2 GB RAM. Obtained signals were subjected to 2D-FFT to generate the wavenumber versus frequency plots shown in Figures 2 and 3. Almost perfect agreement between the simulated – LISA and the analytical solution was observed even for higher modes. EFIT showed less agreement despite the fact that for EFIT a finer grid was used in the model. A convergence of the EFIT solution with the LISA and analytical ones was observed with decreasing cell size, which indicates that the used simulation methods correctly describe Lamb waves' behavior.

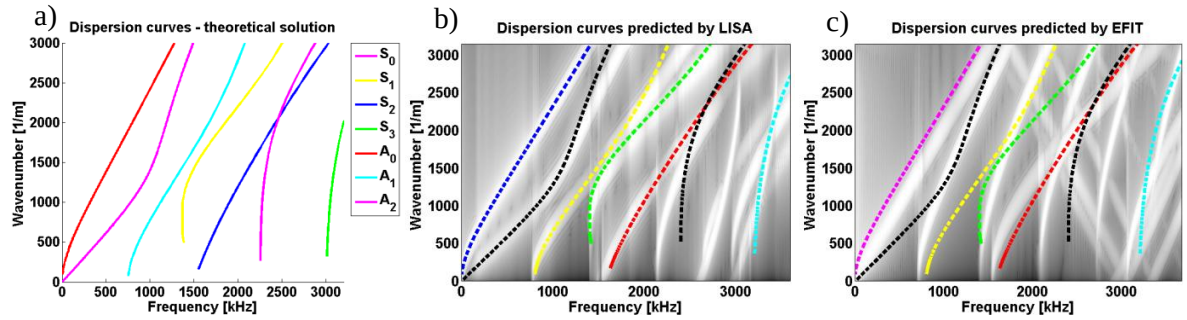

Figure 2. Wavenumber vs. frequency plot obtained by analytical solution (a) and numerical calculation with (b) LISA and (c) EFIT.

In the next step the characteristics obtained from the simulation were validated experimentally. The measurement was performed for 2 mm thick aluminum plate. To acquire the experimental data two PZT transducers of size 5x5x2 mm (Noliac CMAP07) were used in a pitch-catch setup. Wax was used as a coupling agent. The receiving transducer was shifted along 75 mm distance with a step of 1 mm. In Figure 3c can be seen that the S_0 mode is hardly recognizable for the lower wavenumber-frequency range. Similar relation can be observed in the data from simulation (Figure 3a and 3b). In the experiment PZTs transducers were attached to the plate with wax as coupling while in the simulation the assumption on perfect bounding was made, so a slight difference in obtained images can be observed. Note that the increase in amplitude, observed in Figure 3c for all the components around 350 kHz corresponds to the Noliac resonance.

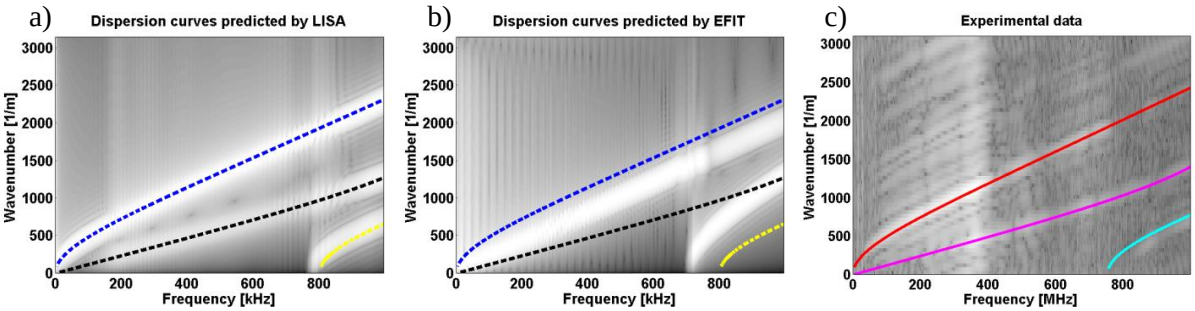

Figure 3. Wavenumber vs. frequency plot obtained by 2D-FFT of simulated signals with (a) LISA and (b) EFIT (c) 2D-FFT of measured signals.

It is worth noting that comparison of the obtained wavenumber-frequency relations between the experimental and simulated data can be used in inverse analysis to identify material parameters.

An example of a designed system

LISA and EFIT simulations were used to facilitate the design of the damage detection system in an aluminum plate. In this example the simulation tool was used for the choice of the excitation frequency and also for investigating the influence of transducers for generating and receiving waves.

Influence of transducer location

Transducers' distribution over the investigated area is important for all damage detection applications. To cite Tse *et al.* (1989) 'Perfect measurements are possible only where the sensor is not there'. A transducer placed on the examined plate distorts not only the measured signal introducing a measurement error (Su and Ye, 2009), but it influences wave propagation in the investigated area producing additional spurious reflections. When baseline-free method is applied these reflections can indicate ghost damage locations.

To illustrate the influence of the transducer location a 2D model of 2 mm thick aluminum plate was implemented. The simulation was performed in two steps: first, only actuator and sensor was present in the structure (Figure 4a), and second an additional passive PZT was added (Figure 4b). It was not used for any measurement; only scattering from this transducer was analyzed. Rectangular transducers with dimensions 5x2 mm were modeled that were bounded to the plate with wax, which was also included in the model. A two step experiment was modeled; in the first step actuator and sensor were coupled to the plate in a pitch-catch configuration. In the second step, an additional passive PZT was attached to the plate. Then the signals obtained in both steps were subtracted from each other and the differences of the signals obtained from the simulation and experiment are shown in Figure 5a and 5b, respectively.

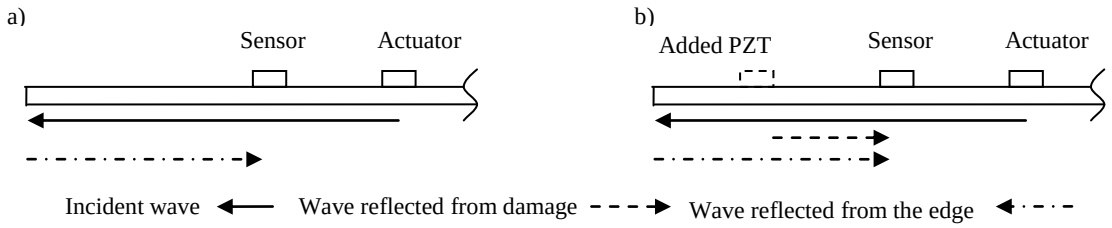

Figure 4. Two scenarios for aluminum plate a) only Actuator and Sensor is used b) additional PZT added to the structure.

The distance of propagation was calculated based on time of flight for identified peaks for group velocity; results are presented in Table 1. For both simulated and experimental data the reflection from additional PZT can be easily identified. In Figure 5 can be seen that the passive PZT located on the wave's way to the plate edge alters shape of the wave reflected from the plate edge. Thus, both the experiment and simulation confirmed that a passive transducer (a small mass) attached to the plate alters wave propagation. The difference can be significant so that the damage detection algorithm may identify the passive transducer as a damaged area.

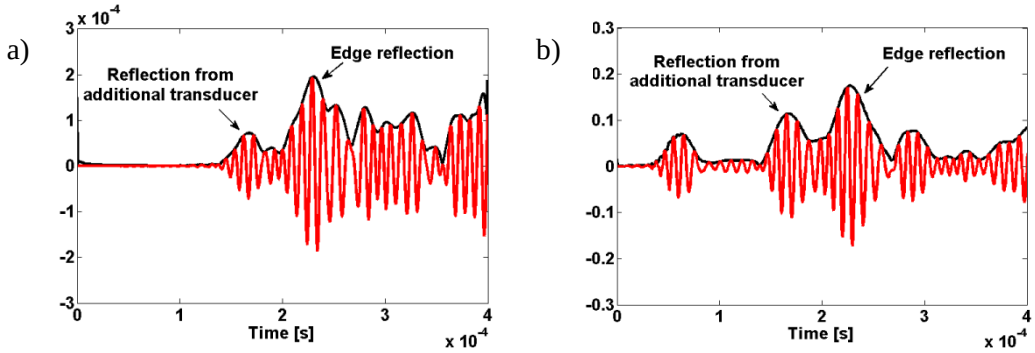

Figure 5. Difference of signals obtained before and after additional PZT was placed (a) simulated data (b) measurement.

Table. 1. Propagation path lengths. A – actuator, S – sensor P – additional PZT.

Path	Path length [mm]				
	Real	Estimated at 100 kHz excitation		Estimated at 150 kHz excitation	
		Experiment	Simulation	Experiment	Simulation
A → S	69.5	69.5	69.5	69.5	69.5
A → P1 → S	261.5	247.8	262	246.3	263
A → edge → S	368.5	360.1	357.4	350.7	349.2

Damage detection method

Damage detection method based on time domain analysis was developed. The procedure (Figure 6) was based on the damage imaging approach presented in (Wang and Yuan, 2009).

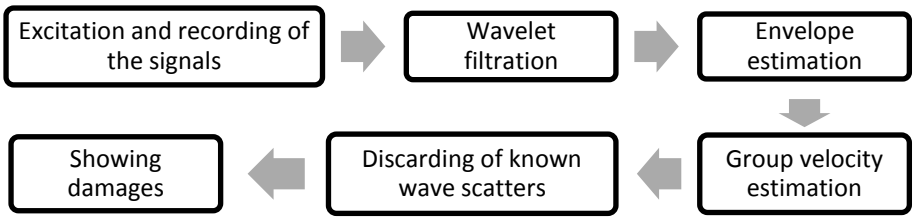

Figure 6. Procedure of damage detection and localization algorithm.

When distributed actuator-sensor grid (Figure 7a) is used there is only a slight difference in time of flight of the incident and scattered wave, moreover as mentioned above, a transducers placed on the structure can influence wave propagation and produce artificial damage locations; thus modified grid (Figure 7b) has been proposed.

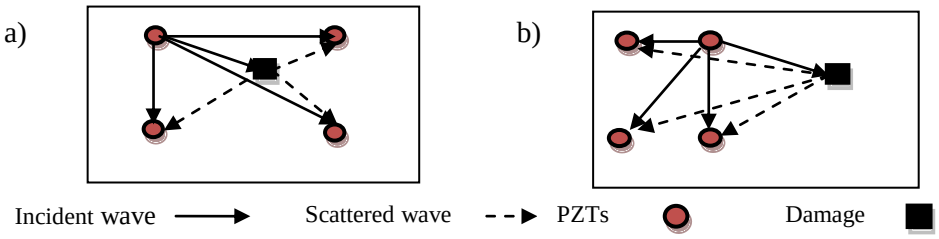

Figure 7. (a) Distributed Pulse-echo grid. (b) Modified actuator-sensor grid.

One pair of actuator – sensor can be active at the same time. The measurement was performed sequentially for all actuator – sensor paths. The acquired signals were subject to wavelet filtration, and then the signal envelope was calculated. Time of flight of the incident wave was extracted and since the distance between PZTs was known, the wave group velocity could be estimated. A square windowing function was applied to signals so scatters from PZTs and edges could be discarded.

Damage localization was performed by representing the investigated area as an image. Next, time of flight that is necessary for wave to travel form actuator to each pixel and back to the sensor was calculated. The value of the pixel $S(i,j)$ was calculated using equation:

$$S(i,j) = \sum_m^N A_m f_{wg}\left(t_{mij}\right) f_m\left(t_{mij}\right),\ m = 1,2 \ldots, N \tag{9}$$

where

$$t_{mij} = \frac{R_m^a + R_m^s}{c_g}, \quad A_m = \frac{10}{max|f_m|}$$

and R_m^a, R_m^s is the distance from damage to actuator and sensor respectively, f_m - envelope of the recorded signal, c_g – group velocity of the wave, f_{wg} – is windowing function. For each actuator–sensor path one image can be obtained. The final result was achieved by summing images from all paths (Wang and Yuan, 2009).

Experimental setup

The object used for the tests was 2 mm thick, 1000 x 1000 mm aluminium plate (EN AW 1050 H14). After introducing a 10x1 mm notch the plate was instrumented with 4 Noliac CMAP07 PZTs transducers of the size 5x5x2 mm with wax as coupling. To satisfy the requirement concerning short time of flight of the incident wave, the transducers were placed at relatively low distance from each other (100 mm as shown in Figure 8a) and formed in a square pattern. The PAQ 16000D instrument (from EC Electronics, Poland) was used as signal generator and data acquisition unit.

In Figure 3 one can see that in low frequency range the S_0 mode is hardly recognizable and the A_0 is a dominant mode, so this mode was selected for damage detection and the presence of the S_0 mode was neglected, as predicted in the simulation.

A 100 kHz Hanning windowed 5 cycle sine was used as an excitation signal and sequential measurements for all actuator-sensor paths were performed. No baseline measurements were performed and dead zones were introduced in the vicinity of the known scatter sources: PZTs placed on the plate and edges. The result of damage imaging is shown in Figure 8.

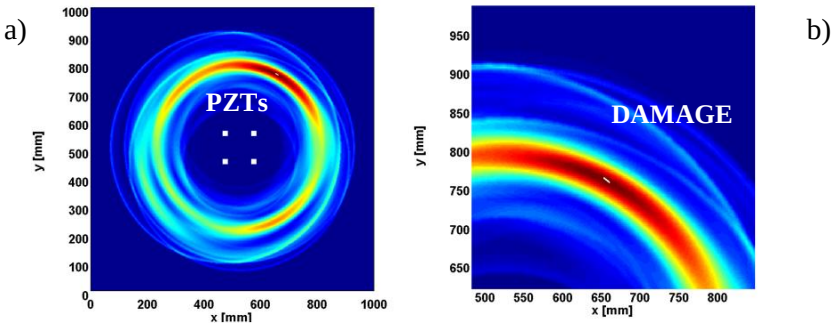

Figure 8. Damage imaging result.

Conclusions

Two different numerical approaches to wave modeling, LISA and EFIT, were presented. The former, which is based on specific application of the finite difference formalism results in a sharp interface model. LISA allows for an accurate modeling of reflection and transmission phenomena at interfaces with large impedance differences. The latter, EFIT, uses staggered grid concept, which eliminates differentiation problems. Investigated Lamb waves were excited by bulk waves interacting with stress – free boundaries of the plate, thus no simplification was introduced. Results of the simulations for both methods are in good agreement with experimental results and the theoretical solutions, and therefore they can serve as a tool for further prediction of Lamb wave phenomena, such as an interaction with damage. Numerical techniques can be combined with measurements to solve an inverse problem of material parameters identification, where the dispersion curves can be used as a reference.

In the presented experimental setup Lamb wave dispersion characteristics obtained from the simulation were helpful in selecting the excitation frequency suitable for the generation of the desired wave mode. The simulations of waves scattered from a passive piezo-transducer attached to the surface facilitated the design of modified transducer grid congested in one area of the plate. When scatters from the grid were discarded it was possible to detect damage.

Further research will be focused on modeling of high frequency waves to allow for the detection of microdamage at material grain boundaries. First steps have already been done with promising results.

As an example, in Figure 9, grain structure with damage modeled at grain boundaries is presented. An excitation using a 1 MHz frequency burst was applied to the structure and wave interaction with damage at micro scale has been analyzed.

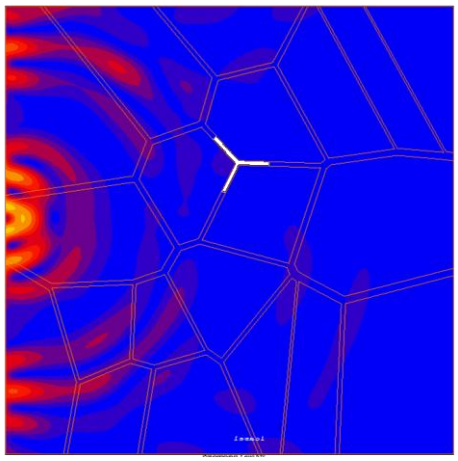

Figure 9. High frequency bulk wave propagation in grain structure of metallic material with damage at grain boundaries.

The proposed tool can be used for adjusting parameters for experimental setup. Also wave distortion due to microcrack can be analyzed and damage size threshold for the particular excitation frequency can be evaluated. The analyzed structures can be simultaneously subjected to a dynamic load and the interaction of wave with propagating damage can be observed.

Acknowledgments

Research funding from the Polish research project MONIT (No. POIG.01.01.02-00-013/08-00) is acknowledged by the authors.

References

Su, Z., L. Ye and Y. Lu (2006), "Guided Lamb waves for identification of damage In composite structures: A review" *Journal of Sound and Vibration*, 295 753–780

Su, Z. and L. Ye (2009), "Identification of Damage Using Lamb Waves From Fundamentals to Applications" *Springer-Verlag Berlin Heidelberg,* pp. 65

Su, Z. and L. Ye (2004), "Selective generation of Lamb wave modes and their propagation characteristics in defective composite laminates. Proceedings of the Institution of Mechanical Engineers Part L" - *Journal of Materials: Design and Applications* 218, 95–110

Giurgiutiu, V (2005), "Tuned Lamb wave excitation and detection with piezoelectric wafer active sensors for structural health monitoring." *Journal of Intelligent Material Systems and Structures* 16, 291–305

Alleyne, D. and P. Cawley (1991), "A two-dimensional Fourier transform method for the measurement of propagating multimode signals" Journal of the Acoustical Society of America 89(3) pp.1159-1168.

Tse, F. and I. Morse (1989), "Measurement and Instrumentation Engineering" *Marcel Dekker, Inc*, New York

Delsanto, P.P., R.S. Schechter, H.H. Chaskelis, R.B. Mignogna and R. Kline (1994), "Connection machine simulation of ultrasonic wave propagation in materials. II: The two dimensional case." *Wave Motion* 20, 295-314

Fellinger, P., R. Marklein, K.J. Langenberg and S. Klaholz (1995), Numerical modeling of elastic wave propagation and scattering with EFIT – elastodynamic finite integration technique. Wave Motion 21, 47-66

Wang, Q. and S. Yuan (2009), "Baseline-free damage imaging method for lamb wave based structural health monitoring" *IV ECCOMAS Thematic Conference on Smart Structures and Materials*.